I&EC research
Industrial & Engineering Chemistry Research
pubs.acs.org/IECR
Article

Enhancing CO_2 Absorption with Compact Multiflow Absorber: Evaluation of Operational Factors

Zhenzhen Zhang, Yucong Ge, Li Yang,* Hao Xing, Fang Liu, Xiao Yang, Qingfang Li, and Yi Li

Cite This: *Ind. Eng. Chem. Res.* 2024, 63, 5618−5628
Read Online

ABSTRACT: Innovations in CO_2 absorption devices play a vital role in advancing industrial applications of CO_2 capture; increasing CO_2 absorption rate and decreasing the absorber are important tasks in amine-based CO_2 capture technologies. This study presents a novel absorber, a compact multiflow absorber, which employs cocurrent spray and traditional package. The integrated design of the spray and packed towers reduces the size of the absorber. By incorporating a cocurrent spray tower as the primary absorption unit, the absorber achieves higher CO_2 removal efficiency and significantly cut down the amount of package needed in the traditional absorber. A comparison with reported counter-current spray tower demonstrated higher overall absorption rate for proposed cocurrent spray tower. The cocurrent spray tower has an overall absorption rate approximately 50% higher than the counter-current spray tower in the first 60 s. The new absorber obtained an efficiency at 86%; however, the traditional package is only 67%. The newly designed absorber increased the CO_2 absorption efficiency by 28%. Finally, the relevance of each operational parameter was evaluated through orthogonal tests, while trend analysis elucidated the influence of various factors on the mass transfer evaluation indices.

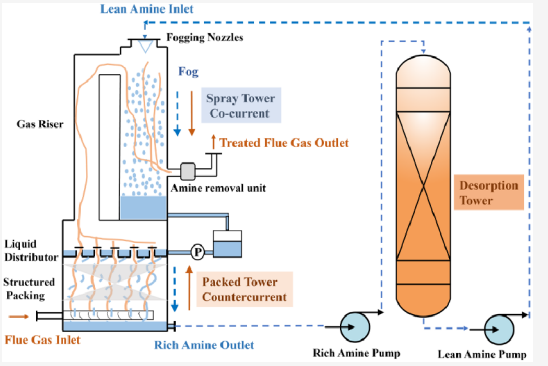

1. INTRODUCTION

CO_2 capture and storage (CCS) can effectively mitigate CO_2 emissions.[1] Postcombustion capture technology is presently a widely utilized and mature technology. Various methods of postcombustion CO_2 capture,[2] such as physicochemical adsorption,[3] membrane separation,[4] cryogenics,[5] chemical looping combustion,[6] and biosequestration,[7] have been explored. Among these, amine-based chemical absorption is currently the most commercially promising CO_2 capture method[8] because of its high purity of separation,[9] high capture rate,[10] and wide range of applications.[11] The success of CO_2 capture via chemical absorption is evident from its application in experimental and pilot-scale operations over the past decades, utilizing equipment such as bubble towers,[12] packed towers,[9] and spray towers.[13] Conventionally, CO_2 capture process is studied in packed towers.[14] Packed towers are susceptible to plugging and have high capital and operating costs due to the packing.[15] Additionally, many researchers have reported that increasing monoethanolamine (MEA) concentrations increased overall gas side mass transfer coefficient ($K_{G\alpha}$).[16] Due to the high viscosity and corrosivity of MEA, high MEA concentrations are avoided in packed towers.[17] Spray towers are less susceptible to corrosion due to the lack of tower internals.[13] They have a lower pressure drop and are less costly if longer residence times are not required.[18] Spray towers lack expensive packing materials, which is expected to result in lower capital costs.[19] Additionally, the absence of internals permits the use of higher MEA concentrations since the corrosion of column internals is avoided.[20] A 12% reduction in reboiler duty by use of 40 wt % MEA instead of 30 wt % MEA has been reported.[21] Despite these advantages, there is a limited number of studies on spray towers in the existing literature.[22]

Recent studies have investigated the CO_2 capture process in spray towers.[23] Kuntz and Aroonwilas pioneered the investigation of CO_2 capture by MEA in a spray tower.[19] In their groundbreaking study, the performance of packed towers and spray towers was meticulously compared, particularly at MEA concentrations reaching up to 43%. The results unveiled a notable 2-7 times higher CO_2 removal rate in the spray tower compared to the packed tower. The efficiency of a spray tower's absorption process hinges significantly on the surface area of the droplets, determined by the size distribution of these droplets.[24] To shed light on this critical aspect, Tamhankar et al. provided experimental data on the particle size distribution of amine spray droplets, offering, for the first time, a quantification of the available surface area through droplet size measurements.[20,25] This analysis revealed that

Received: December 16, 2023
Revised: March 7, 2024
Accepted: March 11, 2024
Published: March 22, 2024

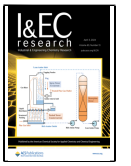

https://doi.org/10.1021/acs.iecr.3c04470
Ind. Eng. Chem. Res. 2024, 63, 5618−5628

while the effect of the inlet load on the planar surface area was not significant, the rate of CO_2 uptake exhibited a strong dependence on the inlet load. In a separate study, an exceptional K_{Ga} value of 11.7 kmol·m^{-3}·kPa^{-1}·h^{-1} was achieved using pure MEA in a spray tower, surpassing values found in the existing literature.[26] This notable enhancement can be attributed to the presence of more MEA in the viscous droplets, countering potential limitations and resulting in higher K_{Ga}. Beyond chemical properties, the design of conventional spray towers also plays a pivotal role in improving system performance. Investigating the impact of cyclonic inlet airflow on K_{Ga}, researchers found an enhancement ranging from 31% to 49% compared to axial inlet airflow.[27] Pilot experiments utilizing three spray towers connected in series provided valuable insights, indicating that lower dynamic viscosity results in faster CO_2 diffusion across the droplet surface, thereby increasing CO_2 uptake.[28] Moreover, employing dual nozzles in a variable-size reactor, directing MEA from both sides, proved to double the total effective area.[29,30] Computational fluid dynamics (CFD) emerged as an indispensable tool for unraveling key properties such as flow field, temperature field, and species profile in spray towers.[31] In a comparative CFD analysis of upward and downward sprinkler schemes, upward spraying was found to mitigate spatial droplet separation, increase droplet residence time and volume fraction, and significantly elevate CO_2 removal from 48.2% to 55.9%.[17] However, despite these advancements, spray towers face challenges related to solvent underutilization due to large droplet sizes and wall flow phenomena. In summary, recent studies underscore the significant improvements in K_{Ga} achieved by spray towers over packed towers. Nonetheless, the persistent issue of low absorption efficiency in spray towers, attributed to insufficient solvent utilization resulting from large droplet sizes and wall flow phenomena, remains a focus of ongoing research and development efforts.

In light of these considerations, the present study is focused on enhancing the CO_2 absorption process through the implementation of a compact multiflow absorber. As shown in Figure 1, the upper part of the absorber is a cocurrent spray tower for CO_2 capture, while the lower part is a packed tower for counter-current flow CO_2 absorption. Solvent passes through the spray and packing sections sequentially under the effect of gravity. CO_2 absorption in the spray tower mainly occurs at the nozzle exit, where a pronounced level of turbulence and rapid disintegration of the liquid sheet or jet occur near the tip of the nozzle. This turbulence significantly accelerates the absorption of CO_2 by the liquid. Moreover, elevated flow rates at the gas inlet can produce a similar effect. The close proximity of the gas inlet to the nozzle in a cocurrent spray tower, in comparison to a counter-current spray tower, results in a heightened gas flow rate in the vicinity of the nozzle. Consequently, increased shear stress is exerted on the droplet surface. This heightened shear stress augments the internal circulation of the liquid, thereby boosting the rate of mass transfer across the liquid film.[32] At high gas velocities, droplets may also oscillate, further enhancing the mass transfer rate compared to nonoscillating droplets. Thus, using cocurrent absorption is a feasible way to enhance absorption performance.[33] The compact multiflow absorber uses a cocurrent spray tower as the primary absorption unit, which absorbs up to 60% of CO_2. The primary absorption solvent then enters the packed tower for secondary absorption, partially absorbing the remaining 40% of CO_2. Since the

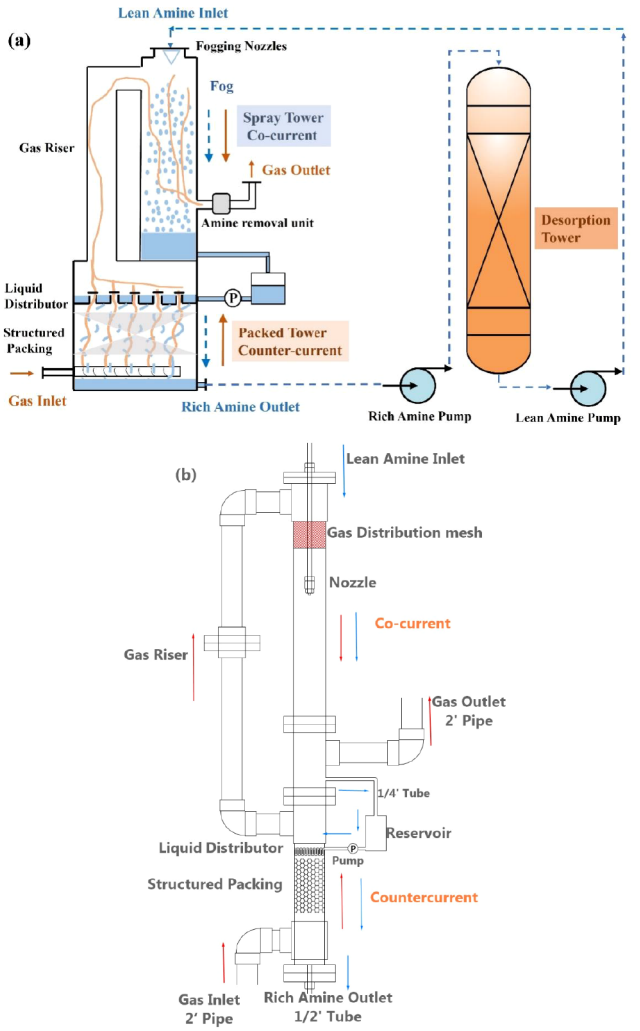

Figure 1. (a) Schematic diagram of compact multiflow absorber; (b) the detailed geometry of proposed compact multiflow absorber.

absorption efficiency of the packed tower is directly proportional to the packing height,[34] absorbing 40% of CO_2 in the packed tower greatly reduces packing usage. This allows for higher concentrations of absorbent for absorption reactions and reduces the corrosion of experimental equipment due to reduced packing usage.

In this study, we compared the CO_2 absorption performance of cocurrent and counter-current spray towers. The absorption effects of packed towers, spray towers, and multiflow absorber were compared, concluding that a multiflow absorber could achieve over 90% absorption efficiency while reducing packing use. This research evaluated the importance of factors (operating parameters) for the proposed compact absorber by conducting orthogonal tests and analyzing the relationship between factors and mass transfer evaluation indices (CO_2 removal efficiency and overall absorption rate). Optimum conditions for different performance evaluation indices were obtained by range analysis, and the degree of influence of each factor on the CO_2 absorption performance was indicated. Trend analysis determined the relationship between the mean value of each factor and the evaluation index. Compared with traditional packed towers, the proposed compact multiflow absorbers have potential application value in achieving higher absorption rates, reducing operating costs by decreasing

https://doi.org/10.1021/acs.iecr.3c04470
Ind. Eng. Chem. Res. 2024, 63, 5618−5628

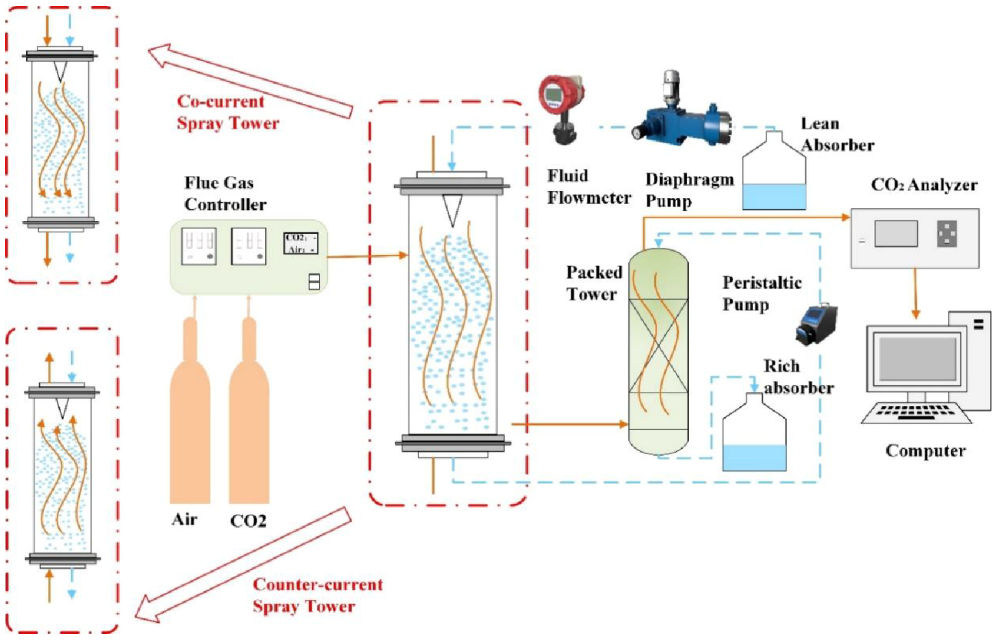

Figure 2. Schematic diagram of CO_2 absorption experimental setup.

packing usage, and reducing the absorber tower's size to minimize the footprint.

2. EXPERIMENTAL SECTION

2.1. Experimental Process. Based on experimental principles, a laboratory-scale test bench was constructed, as depicted in Figure 2. The fluids (liquid and gas) circulated cocurrently or countercurrently within the tower. Transparent acrylic served as the tower body to enable the clear observation of liquid flow. The 1 m high spray tower, with a 0.2 m inner diameter, and the 1 m high packed tower, with a 0.06 m inner diameter, constituted the experimental setup. The mixture flow rate (CO_2 and air) was controlled by a mass flow meter, and the gas volume share was managed through a gas distributor (KT-C2ZK, Zhengzhou Keteng Instrument Co., Ltd.). For precise gas pressure adjustment (ranging between 0.2 and 0.4 MPa) before distribution, a pressure regulator was employed upstream of the gas distributor. The total gas flow within the tower remained constant during the operation. Prior to entering the gas analyzer, gases were dried by using color-changing silica gel. The infrared gas analyzer (Gasboard-3100, Hubei Ruisi Automatic Control Instrument Co., Ltd.) monitored CO_2 concentrations at the inlet and outlet, with a range of 0−20% by volume and a reading accuracy of 0.2% of full scale. To pump liquid into the nozzle, the spray tower utilized a diaphragm pump (J-XM100/1.4, Huaian Kerui Pump Co., Ltd., pressure 0−1.4 MPa, flow rate 0−100 L/h) ensuring accuracy and stability with a connected stainless steel diaphragm-type pulse damper. Liquid flow was measured using a gear flowmeter (GF08, Shanghai Shinyu Precision Machinery Co., Ltd., accuracy ±5%). Nozzles with a 1.1 mm diameter were introduced through the top central opening of the spray tower, secured by a stainless steel ferrule to the geometric center of the column. The packed tower incorporated 250Y stainless steel gauged packing. The solvent from the spray tower was directed into the packed tower via a peristaltic pump (BF600C). Initially, CO_2 and air gas were thoroughly blown through the reactor, and the CO_2 percentage at the reactor outlet was continuously recorded. For safety and measurement consistency, MEA was introduced into the reactor once a consistent CO_2 concentration was observed at the inlet and outlet. At the experiment's conclusion, a run with ultrapure water in the feed tank was conducted to clean all devices.

The flow sequence for both the parallel-flow spray tower and the counterflow packed tower experiments is as follows: The solvent process initiates with the preparation of a lean liquid, which is stored in the lean liquid tank. The lean liquid is then sequentially pumped through the diaphragm pump, damper, and flow meter before entering the nozzle situated at the top of the spray tower. Within the spray tower, the solvent undergoes atomization through the nozzle, resulting in the formation of fine droplets. These liquid droplets engage in parallel-flow contact with the flue gas as they exit from the bottom of the spray tower. Subsequently, the solvent is directed to the top of the packed tower via a peristaltic pump. Inside the packed tower, the solvent engages in a counter-current flow interaction with flue gases before exiting from the bottom of the tower and ultimately entering the rich liquid tank. The flue gas flow is as follows: CO_2 and air are introduced through a gas distributor at the top of the spray tower. The flue gas undergoes parallel-flow contact with the solvent within the spray tower and exits the mixture from the bottom. The gas then enters the packed tower, engaging in counter-current contact with the solvent. Finally, the fully reacted flue gas is subjected to drying using color-changing silica gel before entering the CO_2 gas analyzer.

2.2. Orthogonal Design of Experiments. To analyze the effects of the MEA concentration (Factor A), liquid flow rate (Factor B), CO_2 concentration (Factor C), and total gas flow rate (Factor D) on the CO_2 absorption performance, an orthogonal experimental design method was employed. As shown in Table 1, each factor had four levels of variation: 10, 20, 30, and 35 wt % for MEA concentration; 300, 400, 500, and 600 mL/min for liquid flow rate; 8 vol %, 10 vol %, 12 vol %, and 14 vol % for CO_2 concentration; and total gas flow rates of 25, 30, 35, and 40 L/min. The orthogonal design Table $L16(4^5)$, presented in Table 2, is an array of 4 factors with 4

https://doi.org/10.1021/acs.iecr.3c04470
Ind. Eng. Chem. Res. 2024, 63, 5618−5628

Table 1. Factor Level Table

level	MEA concentration (wt %)	liquid flow rate mL/min	CO_2 concentration (vol %)	total gas flow rate (L/min)
1	10	300	8	25
2	20	400	10	40
3	30	500	12	30
4	35	600	14	35

Table 2. Orthogonal Experimental Design Factors and Levels for Compact Multiflow Absorber

	factor				levels			
exp. number	A	B	C	D	A (wt %)	B (mL/min)	C (vol %)	D (L/min)
1	1	1	1	1	10	300	8	25
2	1	2	2	4	10	400	10	40
3	1	3	3	2	10	500	12	30
4	1	4	4	3	10	600	14	35
5	2	1	2	3	20	300	10	35
6	2	2	1	2	20	400	8	30
7	2	3	4	4	20	500	14	40
8	2	4	3	1	20	600	12	25
9	3	1	3	4	30	300	12	40
10	3	2	4	1	30	400	14	25
11	3	3	1	3	30	500	8	35
12	3	4	2	2	30	600	10	30
13	4	1	4	2	35	300	14	30
14	4	2	3	3	35	400	12	35
15	4	3	2	1	35	500	10	25
16	4	4	1	4	35	600	8	40

levels for each factor. CO_2 removal efficiency (η) and overall absorption rate (Φ) served as evaluation indices. The results of the orthogonal test were analyzed by using range analysis to determine the optimal operating conditions and their degree of influence. Orthogonal tests and subsequent data analysis were employed to ascertain the optimum process conditions.

2.3. Range Analysis. Range analysis, also known as the intuitive analysis method, is commonly used for analyzing the results of orthogonal experiments. The principle behind this analysis is that orthogonal tests exhibit orthogonality and comprehensive comparability, allowing for changes in the average among different factor levels to be considered as the effects of these levels. The extreme differences in factor averages for a particular factor can be viewed as the overall experimental effect of that factor, with larger values indicating a higher importance in the experiment. The calculation involves computing the K_{jm} and R_j values. K_{jm} represents the sum of experimental results at level m (m = 1, 2, 3, 4) for factor j (j = A, B, C, D). K_{jm} mean value is utilized to calculate the R_j value. R_j value, the extreme deviation value, is the largest mean K_j value subtracted from the smallest mean K_j value and is employed for determining the primary and secondary factors' order.

$$K_{A1} = \eta_1 + \eta_2 + \eta_3 + \eta_4 \quad (1)$$

$$K_{A2} = \eta_5 + \eta_6 + \eta_7 + \eta_8 \quad (2)$$

$$K_{A3} = \eta_9 + \eta_{10} + \eta_{11} + \eta_{12} \quad (3)$$

$$K_{A4} = \eta_{13} + \eta_{14} + \eta_{15} + \eta_{16} \quad (4)$$

$$k_{A1} = \frac{K_{A1}}{4} \quad (5)$$

$$k_{A2} = \frac{K_{A2}}{4} \quad (6)$$

$$k_{A3} = \frac{K_{A3}}{4} \quad (7)$$

$$k_{A4} = \frac{K_{A4}}{4} \quad (8)$$

$$R_j = \max(k_{Am}) - \min(k_{Am}) \quad (9)$$

where η_i is the calculated CO_2 removal efficiency for the number of experiments i. The overall absorption rate Φ can be obtained by a similar procedure.

3. REACTION MECHANISMS AND MASS TRANSFER MODELS

3.1. Absorption Reaction Mechanism. The interaction between an alcoholamine solution and CO_2 adheres to the two-film theory, as illustrated in Figure 3, providing a schematic representation of mass transfer within a liquid membrane reaction.[35] The initial step involves the diffusion of CO_2 from the gas phase to the gas−liquid interface, where it encounters the alcoholamine solution. The ensuing reaction between CO_2 and the alcoholamine solution operates in a fast reaction mode, wherein all of the CO_2 molecules react exclusively within the liquid film and do not reach the liquid phase. Following the reaction, the resulting product diffuses to the opposite side of the liquid film. The diffusion rate is contingent upon the molecular diffusion coefficient and the concentration gradient of the substance. Equation 10 and eq 11 are instrumental in defining the liquid CO_2 flux, utilizing the partial pressure driving force and overall mass transfer coefficient, respectively. Equation 12 further articulates the chemical-liquid side mass transfer coefficient (k_g') in terms of partial pressure driving units.

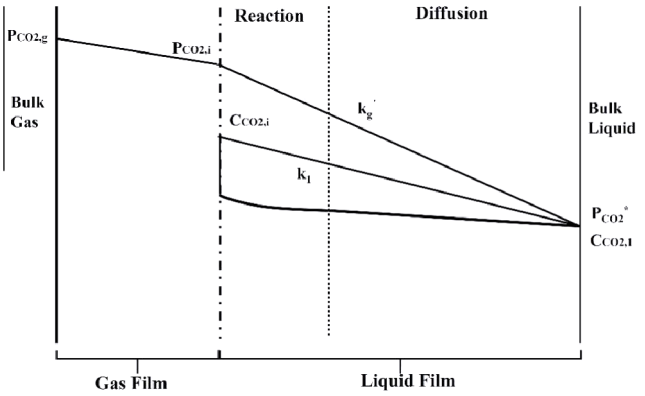

Figure 3. Film theory representation of mass transfer with chemical reaction[35] (reproduced or adapted with permission from ref 35. Copyright 2015 Elsevier).

$$N_{CO_2} = \frac{Ek_l^\circ}{H_{CO_2}}(P_{CO_2,i} - P_{CO_2}^*) \quad (10)$$

https://doi.org/10.1021/acs.iecr.3c04470
Ind. Eng. Chem. Res. 2024, 63, 5618−5628

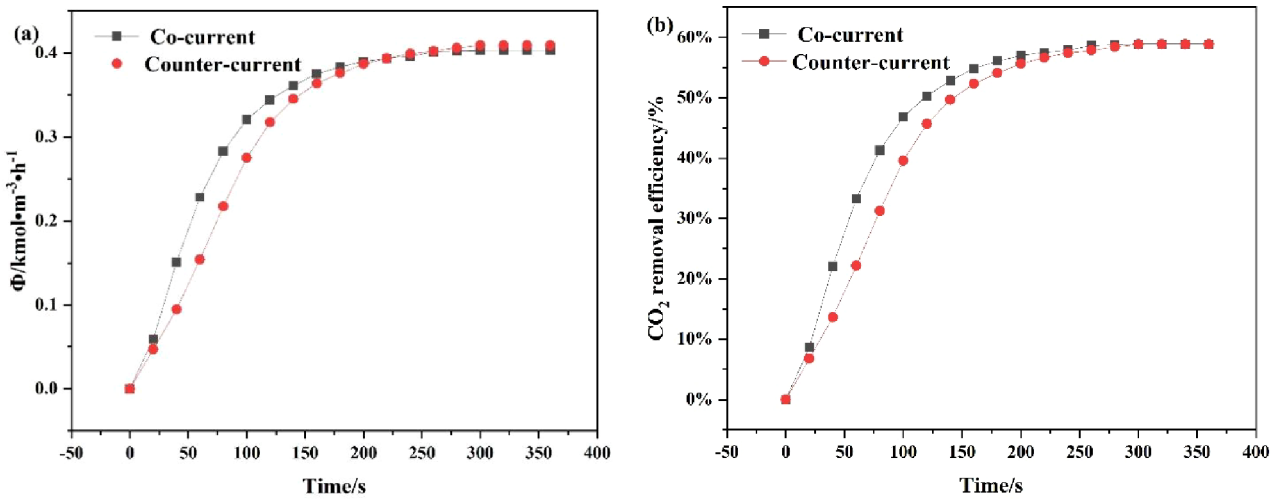

Figure 4. CO_2 absorption performance in different flow configurations. (a) Overall absorption rate and (b) CO_2 removal efficiency.

$$\frac{1}{K_G} = \frac{1}{k_g} + \frac{H_{CO_2}}{Ek_l^o} \tag{11}$$

$$k_g' = \frac{Ek_l^o}{H_{CO_2}} \tag{12}$$

where N_{CO_2} is CO_2 flux(kmol/min); E is enhancement factor; k_l^o is physical local liquid side mass transfer coefficient(m/min); H_{CO_2} is Henry's constant for CO_2 in solvent (m^3·atm/kmol); P_{CO_2} is partial pressure of CO_2 (atm; where i is bin in dropsize measurement or interface in film theory, * is equilibrium, g is gas); K_G is overall gas side mass transfer coefficient (kmol/m^2·min·atm); k_g is local gas side mass transfer coefficient (kmol/m^2·min·atm); k_g' is local liquid side mass transfer coefficient in gas units (kmol/m^2·min·atm); C_{CO_2} is concentration of CO_2 in the solution (kmol/m^3; where l is liquid).

The reaction of CO_2 absorption by alcoholic amine absorbents is generally considered to follow the zwitterion mechanism,[36] first proposed by Caplow et al. in 1968. This mechanism provides a clear explanation for the reaction between an alcoholamine solution and CO_2. According to the zwitterion mechanism, the reaction of alcoholamines with CO_2 occurs in two steps.[37] The first step involves the reaction of CO_2 with the amine solution (RNH_2) to form the zwitterion intermediate ($RNH^{2+}COO^-$), as shown in eq 13. This intermediate then undergoes a deprotonation reaction with any base (B) in the system, forming the carbamate ion and the protonated base (B^+), as illustrated by eq 14. The first step is a rate control step as it is a secondary reaction, while the second step is often recognized as an instantaneous reaction. From the reaction mechanism described above, we can conclude that there are two main products for the reaction of CO_2 with MEA: carbamate and bicarbonate.[38] Equations 15−19 show the specific reactions of CO_2 with MEA.

$$CO_2 + RNH_2 \rightleftarrows RNH_2{}^+COO^- \tag{13}$$

$$RNH_2{}^+COO^- + B \rightleftarrows B^+ + RNHCOO^- \tag{14}$$

$$2H_2O \rightleftarrows H_3O^+ + OH^- \tag{15}$$

$$CO_2 + 2H_2O \rightleftarrows H_3O^+ + HCO_3{}^- \tag{16}$$

$$HCO_3{}^- + H_2O \rightleftarrows CO_3{}^{2-} + H_3O^+ \tag{17}$$

$$MEAH^+ + H_2O \rightleftarrows MEA + H_3O^+ \tag{18}$$

$$MEACOO^- + H_2O \rightleftarrows MEA + HCO_3{}^- \tag{19}$$

3.2. Mass Transfer Model. *3.2.1. CO_2 Removal Efficiency.* The CO_2 removal efficiency is defined as the ratio of the difference in the CO_2 concentration between the inlet and outlet during the absorption process to the inlet concentration. This efficiency is calculated using the following equation, which takes into account the initial CO_2 concentration at the inlet and the final CO_2 concentration at equilibrium:

$$\eta = \frac{y_i - y_o}{y_i} \times 100\% \tag{20}$$

where η is the CO_2 removal efficiency; y_i is the CO_2 concentration at the absorber tower's inlet, set during the experiment; y_o is the CO_2 concentration at the absorber tower's outlet when equilibrium is reached, measured by a CO_2 analyzer at the gas outlet.

3.2.2. Overall Absorption Rate. The overall absorption rate, defined as the specific absorption flux per unit volume of the liquid phase, is another important factor for evaluating the performance of an absorption tower.[39] The calculation formula for the overall absorption rate is as follows:

$$\phi = \frac{q_G(Y_1 - Y_2)}{V_r} \tag{21}$$

where Φ is the overall absorption rate (kmol/m^3·h); Y_1 is the molar ratio of gas-phase CO_2 at the absorber's inlet (mol/%); Y_2 is the molar ratio of gas-phase CO_2 at the absorber's outlet (mol/%); V_r represents the absorber's volume (m^3); and q_G refers to the molar flow rate of the gas (kmol/h).

4. RESULTS AND DISCUSSION

4.1. Comparative Analysis of Cocurrent and Counter-Current Spray Tower. Co-current and counter-current spray tests were conducted in a 1 m high, 0.2 m diameter spray tower. As shown in Figure 4, both methods achieved maximum

https://doi.org/10.1021/acs.iecr.3c04470
Ind. Eng. Chem. Res. 2024, 63, 5618−5628

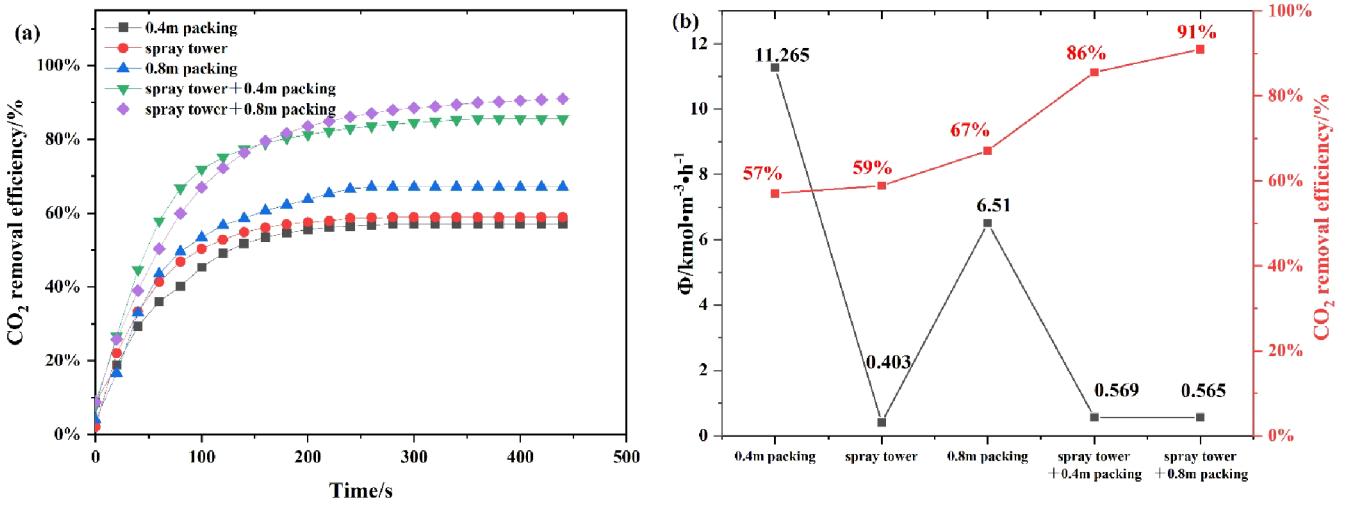

Figure 5. CO_2 absorption performance. (a) CO_2 removal efficiency with time; (b) overall absorption rate and CO_2 removal efficiency.

absorption efficiencies of approximately 60%, demonstrating their equal effectiveness. A comparison with reported counter-current spray tower demonstrated higher overall absorption rate for proposed cocurrent spray tower. Specifically, the cocurrent spray tower exhibited an overall absorption rate approximately 50% higher than the counter-current spray tower within the initial 60 s. This superiority persisted until the 120 s mark, highlighting a consistent advantage in overall absorption rate for the cocurrent absorption tower. This outcome can be attributed to the varying distances between the nozzles and the gas inlets in the cocurrent and counter-current spray towers.

In cocurrent spray towers, the nozzle's proximity to the gas inlet results in substantial mass transfer occurring near the spray nozzle. There is a high degree of turbulence and rapid breakup of the liquid sheet or jet in the area near the tip of the nozzle. Tamhankar et al.,[20] in their study of CO_2 absorption by MEA, emphasized a significant mass transfer occurrence immediately downstream of the nozzle tip. This region is characterized by heightened turbulence, leading to swift absorption of CO_2 from the liquid. Moreover, closer proximity to the nozzle results in smaller droplet sizes, known for their effectiveness in absorption. Studies have shown a consistent and continuous growth trend in measured droplet sizes within the range of 3 to 13 cm from the nozzle, with the rate of growth exceeding 100%.[40] Elevated gas flow rates at the inlet can also impact droplet behavior, causing oscillation at high gas velocities and subsequently increasing the mass transfer rate compared to nonoscillating droplets. The closer gas inlet proximity to the nozzle in a cocurrent spray tower, as opposed to a counter-current spray tower, results in a higher gas flow rate near the nozzle. Consequently, increased shear stress on the droplet surface enhances the internal circulation of the liquid, thereby augmenting the rate of mass transfer across the liquid film.[32] Similar findings have been reported by Bouzin-Turpin et al.[41] In summary, the cocurrent spray tower, with its closer gas inlet proximity to the nozzle, exhibits a higher concentration of flue gas in the vicinity of the nozzle. This spatial arrangement contributes to a significant increase in mass transfer, consequently elevating the rate of CO_2 absorption compared to the counter-current spray tower.

4.2. Comparative Analysis of Multiflow Absorber. To investigate the absorption performance of the proposed multifluid absorption tower, experiments were conducted with the following conditions: 30 wt % MEA concentration, 450 mL/min liquid flow rate, 8 vol % CO_2 concentration, and 25 L/min total gas flow rate. As demonstrated in Figure 5, the 0.4 m packing has an absorption rate of 57%, while the 0.8 m packing has an absorption rate of 67%, resulting in an improvement in absorption efficiency of nearly 18%. Introducing a spray tower to the packing tower, filled with 0.4 m packing, elevated the absorption efficiency to 86%, marking an improvement of almost 51%. The absorption rate of the spray +0.4 m packing configuration is significantly greater than that of the 0.8 m packing alone. However, in terms of the total removal rate, the packed tower exhibited a significantly higher total removal rate than the spray tower. This discrepancy may stem from the swift reduction in interfacial area due to droplet aggregation and liquid film formation on the spray tower wall, leading to a lower mass transfer rate to the spray tower.[27] Additionally, the structural design of the spray tower and inappropriate operating parameters can affect the total removal rate of the spray tower.

For the compact multiflow absorber unit planned for a later stage, it is possible to have the spray tower absorb 60% of the CO_2, and the packed tower absorb the remaining 40%. This design minimizes equipment costs by reducing packing usage while achieving maximum absorption efficiency since the packing in the packed tower constitutes the largest part of the equipment operating cost. Furthermore, this configuration can decrease the size of the absorption tower and its footprint, making it more suitable for industrial applications.

4.3. Range Analysis. Previous experimental investigations predominantly focused on the impact of operating parameters, such as the MEA concentration, liquid flow rate, CO_2 concentration, and total gas flow rate, on the CO_2 capture performance using a univariate experimental approach. These studies paid little attention to the extent to which these factors influenced capture performance. This study aims to assess the importance of each factor (operating parameter) in the proposed compact multiflow absorber design through orthogonal experiments and analyze the relationship between each factor and mass transfer evaluation indices (CO_2 removal efficiency and overall absorption rate). Table S1 shows the orthogonal experiment results for the compact multiflow absorber.

https://doi.org/10.1021/acs.iecr.3c04470
Ind. Eng. Chem. Res. 2024, 63, 5618−5628

Based on the orthogonal experimental chart L16 (4^5) generated from SPSS software, 16 experiments were conducted on the absorber. The results of the CO_2 removal efficiency and overall absorption rate analysis are displayed in Tables S2 and S3. The higher the mean value (k_{ji}) for each factor, the greater the effect that level has on the evaluation indicators, according to the range analysis principle in orthogonal experiments.[42] Range (R_j) indicates the factor's significance, with higher R_j values representing a more substantial impact on metrics. CO_2 removal efficiency and overall absorption rate serve as evaluation indices for the compact multiflow absorber. Figure 6 displays the range analysis of each factor's impact on the two

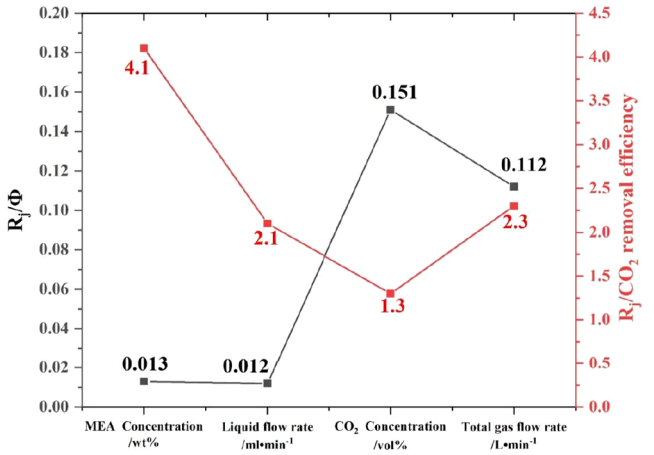

Figure 6. Range analysis of overall absorption rate and CO_2 removal efficiency.

evaluation indices. Based on the range analysis, the primary and secondary order of factors is determined, and the order of each factor's influence on the evaluation indicators is ascertained. When the mean values of the factors are compared, the specific effect of factors on the results is revealed, which helps in determining the optimum combination of factors for maximum performance.

The experimental results in Table S2 show that the CO_2 removal efficiency varies from 91.66% to 99.43%. Examining the range values of different factors reveals the significance level of each factor on the CO_2 removal efficiency: liquid concentration > gas flow rate > liquid flow rate > CO_2 concentration. According to the results in Table S3, the overall absorption rate ranged between 0.14 and 0.4 kmol·m^{-3}·h^{-1}. Examining the range values of different factors provides the significance level of the factors on the overall absorption rate as follows: CO_2 concentration > total gas flow rate > liquid concentration > liquid flow rate. From the above importance ranking, it can be obtained that the MEA concentration has the greatest effect on the CO_2 removal efficiency, while the CO_2 concentration has the greatest effect on the total CO_2 removal rate. Wu et al.[29] evaluated the proposed variable diameter spray tower system by orthogonal tests and similarly found that MEA concentration is a key parameter affecting the CO_2 removal efficiency, with small changes in CO_2 concentration significantly altering the total absorption rate. Similarly, Liao et al.[43] investigated the mass transfer performance of a laboratory-scale structured packed absorber for absorption of CO_2 into a DEEA/MEA mixture. The CO_2 lean load and the CO_2 partial pressure were found to be important factors affecting the total volumetric mass transfer coefficient through orthogonal experiments.

In conclusion, the CO_2 concentration and total gas flow rate have the most significant impact on the overall absorption rate, while the MEA concentration and liquid flow rate are less influential. The highest overall absorption rate was achieved at the following conditions within the range of the experiment: 20 wt % MEA concentration, 300 mL/min liquid flow rate, 14 vol % CO_2 concentration, and 40 L/min gas flow rate, which represents the optimal combination for maximizing overall absorption rate.

Considering the significance level, both the CO_2 removal efficiency and overall absorption rate cannot be simultaneously maximized in the same set of experiments. Thus, a balance should be sought between the roles of each factor when selecting experimental conditions. Liquid concentration was the most critical factor affecting the CO_2 removal efficiency, while the CO_2 concentration was the most important factor affecting the overall absorption rate. Additionally, the MEA flow rate had a minor effect on both evaluation metrics, whereas the total gas flow rate was the second most significant influence on both metrics. Therefore, to achieve higher CO_2 removal and overall absorption rates simultaneously, the experiment should primarily adjust the MEA concentration and CO_2 concentration, followed by the total gas flow rate, and finally the liquid flow rate.

4.4. Trend Analysis of CO_2 Absorption. *4.4.1. Effects of MEA Concentration.* As illustrated in Figure 7, the CO_2

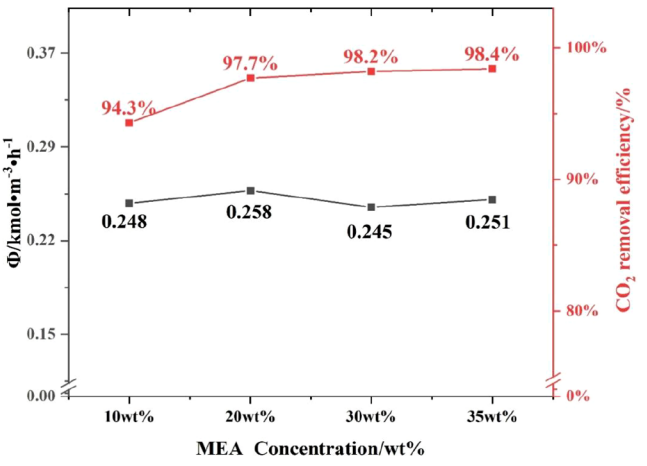

Figure 7. Effect of MEA concentration on the CO_2 removal efficiency and overall absorption rate.

removal efficiency increases linearly with the rise in MEA concentration. Consistent with these findings, Heidaryan et al.[44] captured CO_2 in a continuously oscillating folded plate reactor and similarly found that CO_2 removal efficiency was proportional to amine concentration. This correlation can be attributed to the nature of the absorption of CO_2 by MEA, predominantly occurring in a liquid membrane. The mass transfer interface area and the quantity of free MEA available at the interface determine the CO_2 uptake. As the concentration of MEA increases, a higher number of MEA molecules are present at the interface, leading to an augmentation in CO_2 removal efficiency.[26] For capturing more CO_2, each MEA molecule must enhance either the interfacial area or the circulation within the droplet. Under these circumstances, the more reactive MEA molecules tend to diffuse toward the gas−

https://doi.org/10.1021/acs.iecr.3c04470
Ind. Eng. Chem. Res. 2024, 63, 5618−5628

liquid surface, reacting with CO_2 molecules and increasing the enhancement factor, which in turn raises the absorption rate.[27] Consequently, the CO_2 removal efficiency and overall absorption rate increase accordingly. Furthermore, the rise in MEA concentration showed a minimal impact on the total CO_2 removal rate, ranging from 0.248 kmol·m^{-3}·h^{-1} to 0.258 kmol·m^{-3}·h^{-1}, with an overall slightly increasing trend. This observation aligns with the outcomes of the extreme variance analysis presented in Section 4.3.

However, in conventional packed towers, elevated MEA concentrations result in increased solution viscosity,[45] which can cause severe corrosion problems in the equipment and limit its use in industrial applications.[46] These adverse effects can impair the improvement of the absorption performance and increase the capital cost of maintenance. Therefore, when increasing the MEA concentration in conventional packed towers, it is essential to strike a balance between absorption performance and operating costs.[28] In contrast, the spray-tower-based absorption tower proposed in this study circumvents this issue due to the absence of packing, improving absorption efficiency while reducing the corrosion effect.

4.4.2. Effects of Liquid Flow Rate. Figure 8 displays the impact of the liquid flow rate on the CO_2 removal efficiency and total absorption rate. As the liquid flow rate increases, the CO_2 removal efficiency rises linearly. This is because an increased flow rate results in more MEA molecules for each CO_2 molecule, providing opportunities for absorption. Additionally, the resistance to gas diffusion into the liquid phase decreases as the droplet flow rate increases and the liquid-phase boundary layer gets reduced. Thus, the CO_2 removal efficiency and overall absorption rate increase with an increasing liquid flow rate. Wu et al.[29] observed a similar trend in a variable-diameter spray tower, noting that CO_2 removal efficiency increased with higher liquid flow rates. The authors attributed this phenomenon to the enhanced dispersion of the absorbent in variable-diameter space. As the liquid flow rate increased, the nozzle fragmented the solution into numerous small droplets, thereby enlarging the effective interfacial area between the liquid and gas phases.

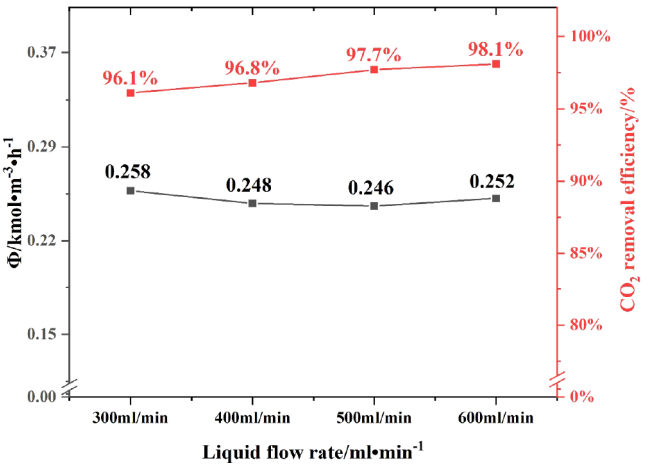

Figure 8. Effect of liquid flow rate on CO_2 removal efficiency and overall absorption rate.

Nevertheless, a gradual decrease in the rate of increase is observed at higher liquid flow rates due to the limitation of increasing the effective interfacial area caused by the reduction in droplet size. As a result, the mass transfer performance does not improve further at higher fluid flow rates.[47] A comparable trend has been reported in previous studies of CO_2 absorption in spray towers.[48] As shown in Figure 8, the overall absorption rate varies with the changing flow rate within the measuring range but only slightly. The effect of liquid flow on the removal of CO_2 is less significant than the effect of the MEA concentration. For the overall absorption rate, the liquid flow rate has a more significant impact than the MEA concentration, as variations in overall absorption rate are more considerable when the liquid flow rate changes. This observation aligns with the results of the range analysis presented in Table S2 for the CO_2 removal efficiency of the compact multiflow absorber and Table S3 for the overall absorption rate. Xu et al.[47] conducted numerical simulations on spray towers and observed that the mass transfer performance does not exhibit further improvement at elevated liquid flow rates. This plateau in performance is attributed to the inhomogeneous interfacial distribution that occurs at higher liquid flow rates. A similar trend was found in previous studies by Kies et al.[48] and Fu et al.[49] in the case of CO_2 uptake by the tower.

4.4.3. Effects of CO_2 Concentration. The experimental findings presented in Figure 9 reveal a consistent decline in the CO_2 removal efficiency with an increase in the CO_2 concentration. This observation aligns with the results of a study by Li et al.,[50] where the CO_2 trapping performance of MEA and NaOH solutions was explored using an air atomization column. The similarity in outcomes suggests that higher CO_2 concentrations correlate with a reduced CO_2 removal efficiency. This phenomenon can be attributed to the increased amount of CO_2 within the same volume of MEA, resulting in a decline in the molar ratio of MEA to CO_2 as the CO_2 concentrations elevate. As the CO_2 concentration increases, the concentration driving force also increases, leading to a higher rate of CO_2 transfer from gas to liquid. This effect indicates that the mass transfer performance is primarily limited by liquid-phase resistance.

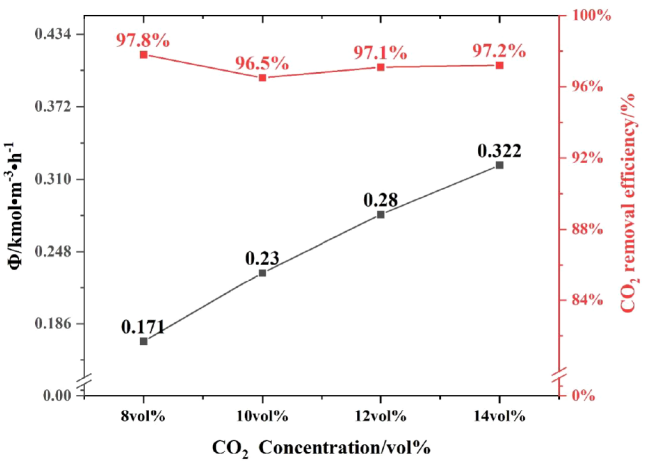

Figure 9. Effect of CO_2 concentration on CO_2 removal efficiency and overall absorption rate.

Nevertheless, the data in Figure 9 reveal a notable upswing in the overall removal rate with an increasing CO_2 concentration. A study by Wu et al.[29] delved into the CO_2 capture performance of MEA solution in a variable diameter spray tower, echoing the finding that CO_2 concentration exerts

https://doi.org/10.1021/acs.iecr.3c04470
Ind. Eng. Chem. Res. 2024, 63, 5618−5628

opposing effects on CO_2 removal efficiency and overall absorption rate. According to dual membrane theory, the driving force of the gas phase and the mass transfer coefficient of the gas phase escalate with increasing CO_2 concentration, resulting in an increase in the overall absorption rate. Conversely, the molar ratio of MEA to CO_2 decreases with the rise in the CO_2 concentration, suggesting that more CO_2 molecules react with a limited number of active MEA molecules. Hence, maintaining the CO_2 concentration at an optimal level becomes imperative for achieving the highest CO_2 removal efficiency and overall absorption rate.

4.4.4. Effects of Total Gas Flow Rate. As shown in Figure 10, the overall absorption rate increases, while CO_2 removal

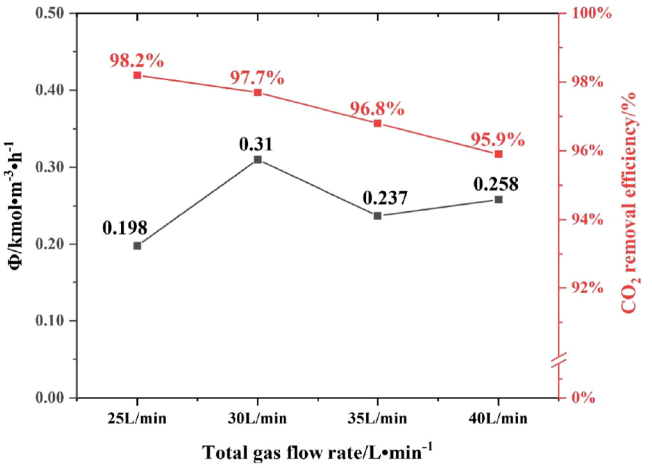

Figure 10. Effect of total gas flow rate on CO_2 removal efficiency and overall absorption rate.

decreases as the gas flow rate rises. Heidaryan et al.[44] similarly found this trend in CO_2 uptake experiments. This trend aligns with the gas−liquid mass transfer theory, which states that the mass transfer coefficient increases with the gas flow rate. As the gas flow rate increases, the liquid to gas ratio decreases, suggesting that the contact between excess flue gas and the finite absorber reduces CO_2 removal. This is because as the gas flow rate increases, the amount of MEA available for each CO_2 molecule decreases for the same liquid flow rate. Chaotic advection of the gas phase intensifies as gas flow rate increases. Consequently, by increasing the gas flow rate, mass transfer rate also increases, and mass transfer can be controlled by gas phase resistance. Gas-phase controlled mass transfer occurs only at low liquid residence times and low gas flow rates, while liquid-phase controlled mass transfer takes place at high gas flow rates and when sufficient contact time exists between gas and liquid.[51] Kuntz and Aaronwilas also observed that mass transfer in spray columns was controlled solely by the gas phase at low gas flow rates.[19]

Nevertheless, the graphical representation illustrates that as the gas flow rate increases, the total removal rate reaches its peak at 30 L/min. This may be due to the fact that as gas velocity increases, the shear stress on the droplet surface rises, which can promote internal liquid circulation within a droplet of a certain size or larger, increasing the mass transfer rate across the liquid film. Droplets can also oscillate at high gas velocities, further enhancing the mass transfer rate compared to nonoscillating droplets.[27] On the other hand, as the gas flow rate continues to increase, the amount of CO_2 in the gas phase rises, leading to a decrease in the chemical reaction enhancement factor. This decrease subsequently diminishes the liquid-phase mass transfer coefficient, impeding the mass transfer between the gas and liquid. Consequently, the total removal rate value declines with further increases in gas flow rate.[50] The observed trend of an initial increase and subsequent decrease in the total removal rate with an increase in gas flow rate aligns with the findings of Li et al.[50] and Demontigny et al.[52] Therefore, maintaining an appropriate gas flow rate is crucial to ensuring high CO_2 removal efficiency and overall absorption rate.

5. CONCLUSION

This study proposes a compact multiflow absorber to achieve efficient CO_2 absorption mass transfer. Within the initial 60 s, the cocurrent spray tower exhibits an overall absorption rate approximately 50% higher than that of the counter-current spray tower. The newly designed absorber achieves an efficiency of 86%, surpassing the 67% efficiency of the traditional package and marking a 28% increase in the CO_2 absorption efficiency. Experimental findings demonstrate that the spray tower, serving as the primary absorption unit, captures 60% of CO_2 in the upper section of the absorber, while the packed tower handles the remaining 40% during secondary absorption. Notably, since the absorption efficiency of packed towers is directly proportional to the packing height, the design choice to allocate 40% CO_2 absorption to packed towers significantly reduces the packing requirement. Finally, the importance of each factor in the multiflow absorber system has been assessed using orthogonal testing, and the relationship between each factor and the mass transfer assessment has been evaluated with trend analysis. In summary, compared to traditional packed towers, the proposed compact multiflow absorber offers potential application value in achieving higher absorption rates, reducing operating costs by decreasing the use of packing. On the other hand, the integrated design of the spray and packed towers reduces the size of the absorber, which in turn reduces the footprint.

■ ASSOCIATED CONTENT

Supporting Information

The Supporting Information is available free of charge at https://pubs.acs.org/doi/10.1021/acs.iecr.3c04470.

Orthogonal experiment results and range analysis data (PDF)

■ AUTHOR INFORMATION

Corresponding Author

Li Yang − *School of Low-Carbon Energy and Power Engineering, China University of Mining and Technology, Xuzhou, Jiangsu Province 221116, China;* orcid.org/0000-0003-3493-6096; Phone: +86-17351051006; Email: li.yang@cumt.edu.cn

Authors

Zhenzhen Zhang − *School of Low-Carbon Energy and Power Engineering, China University of Mining and Technology, Xuzhou, Jiangsu Province 221116, China*

Yucong Ge − *School of Low-Carbon Energy and Power Engineering, China University of Mining and Technology, Xuzhou, Jiangsu Province 221116, China*

https://doi.org/10.1021/acs.iecr.3c04470
Ind. Eng. Chem. Res. 2024, 63, 5618−5628

Hao Xing − *School of Low-Carbon Energy and Power Engineering, China University of Mining and Technology, Xuzhou, Jiangsu Province 221116, China*
Fang Liu − *School of Low-Carbon Energy and Power Engineering, China University of Mining and Technology, Xuzhou, Jiangsu Province 221116, China;* orcid.org/0000-0003-1001-3924
Xiao Yang − *School of Low-Carbon Energy and Power Engineering, China University of Mining and Technology, Xuzhou, Jiangsu Province 221116, China*
Qingfang Li − *Sinopec Petroleum Engineering Co., Ltd., Dongying, Shandong Province 257000, China*
Yi Li − *Sinopec Petroleum Engineering Co., Ltd., Dongying, Shandong Province 257000, China*

Complete contact information is available at: https://pubs.acs.org/10.1021/acs.iecr.3c04470

Notes

The authors declare no competing financial interest.

■ ACKNOWLEDGMENTS

This work was supported by National Key Research and Development Program (2022YFE0130000), the Xuzhou City Science and Technology Project (KC23077), and the Fundamental Research Funds for the Central Universities (2023KYJD1005).

■ REFERENCES

(1) Frimpong, R. A.; Nikolic, H.; Pelgen, J.; Ghorbanian, M.; Figueroa, J. D.; Liu, K. L. Evaluation of different solvent performance in a 0.7 MWe pilot scale CO_2 capture unit. *Chem. Eng. Res. Des.* **2019**, *148*, 11−20.
(2) Di Caprio, U.; Wu, M.; Vermeire, F.; Van Gerven, T.; Hellinckx, P.; Waldherr, S.; Kayahan, E.; Leblebici, M. E. Predicting overall mass transfer coefficients of CO_2 capture into monoethanolamine in spray columns with hybrid machine learning. *J. CO2 Util.* **2023**, *70*, 102452.
(3) Ruhaimi, A. H.; Hitam, C. N. C.; Aziz, M. A. A.; Hamid, N. H. A.; Setiabudi, H. D.; Teh, L. P. The role of surface and structural functionalisation on graphene adsorbent nanomaterial for CO_2 adsorption application: Recent progress and future prospects. *Renewable Sustainable Energy Rev.* **2022**, *167*, 112840.
(4) Kunalan, S.; Palanivelu, K. Polymeric composite membranes in carbon dioxide capture process: a review. *Environ. Sci. Pollut. Res.* **2022**, *29* (26), 38735−38767.
(5) Song, C. F.; Liu, Q. L.; Deng, S.; Li, H. L.; Kitamura, Y. Cryogenic-based CO_2 capture technologies: State-of-the-art developments and current challenges. *Renewable Sustainable Energy Rev.* **2019**, *101*, 265−278.
(6) Saqline, S.; Chua, Z. Y.; Liu, W. Coupling chemical looping combustion of solid fuels with advanced steam cycles for CO_2 capture: A process modelling study. *Energy Convers. Manage.* **2021**, *244*, 114455.
(7) Zhu, X.; Rong, J. F.; Chen, H.; He, C. L.; Hu, W. S.; Wang, Q. An informatics-based analysis of developments to date and prospects for the application of microalgae in the biological sequestration of industrial flue gas. *Appl. Microbiol. Biotechnol.* **2016**, *100* (5), 2073−2082.
(8) Chao, C.; Deng, Y. M.; Dewil, R.; Baeyens, J.; Fan, X. F. Post-combustion carbon capture. *Renewable Sustainable Energy Rev.* **2021**, *138*, 110490.
(9) Rochelle, G. T. Amine scrubbing for CO_2 capture. *Science* **2009**, *325* (5948), 1652−1654.
(10) Sun, L. Y.; Xiao, R.; Lin, J. J.; Kong, D. L.; Luo, K.; Fan, J. R. Numerical investigation of a 1MW full-loop chemical looping combustion unit with dual CFB reactors. *Int. J. Greenhouse Gas Control* **2023**, *123*, 103835.
(11) Venkata Anjani Kiran, S.; Ranganathan, P. Computational fluid dynamics simulation of reactive absorption of CO_2 in a structured packed column. *Can. J. Chem. Eng.* **2023**, *101* (11), 6271−6283.
(12) Zhang, B.; Wang, Z. C.; Luo, Y.; Guo, K.; Zheng, L. Y.; Liu, C. J. A mathematical model for single CO_2 bubble motion with mass transfer and surfactant adsorption/desorption in stagnant surfactant solutions. *Sep. Purif. Technol.* **2023**, *308*, 122888.
(13) Cho, M.; Lee, S.; Choi, M.; Lee, J. W. Novel Spray Tower for CO_2 Capture Using Uniform Spray of Monosized Absorbent Droplets. *Ind. Eng. Chem. Res.* **2018**, *57* (8), 3065−3075.
(14) Lu, R. Z.; Li, K. K.; Chen, J.; Yu, H.; Tade, M. CO_2 capture using piperazine-promoted, aqueous ammonia solution: Rate-based modelling and process simulation. *Int. J. Greenhouse Gas Control* **2017**, *65*, 65−75.
(15) Miao, Y.; Kreider, P.; Pommerenck, J.; AuYeung, N. J.; von Jouanne, A.; Jovanovic, G.; Yokochi, A. CO_2 Reduction by Multiple Low-Energy Electric Discharges in a Microstructured Reactor: Experiments and Modeling. *Ind. Eng. Chem. Res.* **2022**, *61* (30), 10756−10765.
(16) Wang, C.; Seibert, A. F.; Rochelle, G. T. Packing characterization: Absorber economic analysis. *Int. J. Greenhouse Gas Control* **2015**, *42*, 124−131.
(17) Xu, Y.; Chen, X. L.; Zhao, Y. L.; Jin, B. S. Modeling and analysis of CO_2 capture by aqueous ammonia + piperazine blended solution in a spray column. *Sep. Purif. Technol.* **2021**, *267*, 118655.
(18) Liu, D. Y.; Liu, W.; Ma, J. L.; Liang, C.; Chen, X. P. Investigation of CO_2 Capture in Three-Dimensional Full-Loop Integrated Bubbling-Transport Bed Adsorber. *Ind. Eng. Chem. Res.* **2023**, *62* (43), 17691−17700.
(19) Kuntz, J.; Aroonwilas, A. Mass-transfer efficiency of a spray column for CO_2 capture by MEA. *Energy Procedia* **2009**, *1* (1), 205−209.
(20) Tamhankar, Y.; King, B.; Whiteley, J.; Cai, T.; McCarley, K.; Resetarits, M.; Aichele, C. Spray absorption of CO_2 into monoethanolamine: Mass transfer coefficients, dropsize, and planar surface area. *Chem. Eng. Res. Des.* **2015**, *104*, 376−389.
(21) Abu-Zahra, M. R. M.; Schneiders, L. H. J.; Niederer, J. P. M.; Feron, P. H. M.; Versteeg, G. F. CO_2 capture from power plants. *Int. J. Greenhouse Gas Control* **2007**, *1* (1), 37−46.
(22) Jafari, M. J.; Matin, A. H.; Rahmati, A.; Azari, M. R.; Omidi, L.; Hosseini, S. S.; Panahi, D. Experimental optimization of a spray tower for ammonia removal. *Atmos. Pollut. Res.* **2018**, *9* (4), 783−790.
(23) Bhati, A.; Bilyaz, S.; Bahadur, V. Analytical first-principles-based model for sprays-based CO_2 capture. *Int. J. Greenhouse Gas Control* **2023**, *128*, 103969.
(24) Kuntz, J.; Aroonwilas, A. Performance of Spray Column for CO_2 Capture Application. *Ind. Eng. Chem. Res.* **2008**, *47*, 145−153.
(25) Tamhankar, Y.; King, B.; Whiteley, R.; Resetarits, M.; Cai, T.; Aichele, C. Aqueous Amine Spray Absorption and Droplet Distribution Data for CO_2 Capture Applications. *Energy Procedia* **2014**, *63*, 293−300.
(26) Kayahan, E.; Caprio, U. D.; Van den Bogaert, A.; Khan, M. N.; Bulut, M.; Braeken, L.; Van Gerven, T.; Leblebici, M. E. A new look to the old solvent: Mass transfer performance and mechanism of CO_2 absorption into pure monoethanolamine in a spray column. *Chem. Eng. Process.* **2023**, *184*, 109285.
(27) Javed, K. H.; Mahmud, T.; Purba, E. The CO_2 capture performance of a high-intensity vortex spray scrubber. *Chem. Eng. J.* **2010**, *162* (2), 448−456.
(28) Zimmermann, S.; Schmid, M.-O.; Klein, B.; Scheffknecht, G. Experimental Studies on Spray Absorption with the Post Combustion CO_2 Capture Pilot-Plant CASPAR. *Energy Procedia* **2017**, *114*, 1325−1333.
(29) Wu, X. M.; Qin, Z.; Yu, Y. S.; Zhang, Z. X. Experimental and numerical study on CO_2 absorption mass transfer enhancement for a diameter-varying spray tower. *Appl. Energy* **2018**, *225*, 367−379.
(30) Wu, X. M.; Sharif, M.; Yu, Y. S.; Chen, L.; Zhang, Z. X.; Wang, G. Hydrodynamic mechanism study of the diameter-varying spray

tower with atomization impinging spray. *Sep. Purif. Technol.* **2021**, *268*, 118608.
(31) Zhao, B. T.; Su, Y. X.; Cui, G. M. Post-combustion CO_2 capture with ammonia by vortex flow-based multistage spraying: Process intensification and performance characteristics. *Energy* **2016**, *102*, 106−117.
(32) Yeh, N. K.; Rochelle, G. T. Liquid-phase mass transfer in spray contactors. *AichE J.* **2003**, *49* (9), 2363−2373.
(33) Koller, M.; Wappel, D.; Trofaier, N.; Gronald, G. Test results of CO_2 spray scrubbing with Monoethanolamine. *Energy Procedia* **2011**, *4*, 1777−1782.
(34) Seyboth, O.; Zimmermann, S.; Heidel, B.; Scheffknecht, G. Development of a Spray Scrubbing Process for Post Combustion CO_2 Capture with Amine Based Solvents. *Energy Procedia* **2014**, *63*, 1667−1677.
(35) Tamhankar, Y.; King, B.; Whiteley, J.; McCarley, K.; Cai, T.; Resetarits, M.; Aichele, C. Interfacial area measurements and surface area quantification for spray absorption. *Sep. Purif. Technol.* **2015**, *156*, 311−320.
(36) Akachuku, A.; Osei, P. A.; Decardi-Nelson, B.; Srisang, W.; Pouryousefi, F.; Ibrahim, H.; Idem, R. Experimental and kinetic study of the catalytic desorption of CO_2 from CO_2-loaded monoethanolamine (MEA) and blended monoethanolamine − Methyl-diethanolamine (MEA-MDEA) solutions. *Energy* **2019**, *179*, 475−489.
(37) Liu, H.; Jiang, X.; Idem, R.; Dong, S.; Tontiwachwuthikul, P. Comprehensive reaction kinetics model of CO_2 absorption into 1-dimethylamino-2-propanol solution. *AichE J.* **2022**, *68* (11), No. e17816.
(38) Li, Z.; Wang, L. L.; Li, C. P.; Cui, Y. N.; Li, S. M.; Yang, G.; Shen, Y. M. Absorption of Carbon Dioxide Using Ethanolamine-Based Deep Eutectic Solvents. *ACS Sustainable Chem. Eng.* **2019**, *7* (12), 10403−10414.
(39) Zeng, Q.; Guo, Y. C.; Niu, Z. Q.; Lin, W. Y. The absorption rate of CO_2 by aqueous ammonia in a packed column. *Fuel Process. Technol.* **2013**, *108*, 76−81.
(40) Li, M.; Yang, H. Z.; Wang, J. J.; Li, G.; Tang, J. An Experimental Investigation of the Impact of Surface Tension and Viscosity on the Atomization Effect of a Solid Cone Nozzle. *Appl. Sci.* **2023**, *13* (7), 4522.
(41) Bouzin-Turpin, A.; Couvert, A.; Laplanche, A.; Paillier, A. Co-current and counter-current spraying of odour-neutralizing products. *Environ. Technol.* **2009**, *30* (14), 1511−1517.
(42) Wu, X. M.; He, M.; Yu, Y. S.; Qin, Z.; Zhang, Z. X. Overall Mass Transfer Coefficient of CO_2 Absorption in a Diameter-varying Spray Tower. *Energy Procedia* **2017**, *114*, 1665−1670.
(43) Liao, H. Y.; Gao, H. X.; Xu, B.; Liang, Z. W. Mass transfer performance studies of aqueous blended DEEA-MEA solution using orthogonal array design in a packed column. *Sep. Purif. Technol.* **2017**, *183*, 117−126.
(44) Heidaryan, E.; Gouran, A.; Nejati, K.; Aghel, B. Enhancement of CO_2 capture operation in oscillatory baffled reactor. *Sep. Purif. Technol.* **2023**, *324*, 124536.
(45) Qing, Z.; Yincheng, G.; Zhenqi, N. Experimental studies on removal capacity of carbon dioxide by a packed reactor and a spray column using aqueous ammonia. *Energy Procedia* **2011**, *4*, 519−524.
(46) Niu, Z. Q.; Guo, Y. C.; Lin, W. Y. Experimental studies on removal of carbon dioxide by aqueous ammonia fine spray. *Sci. China, Ser. E: Technol. Sci.* **2010**, *53* (1), 117−122.
(47) Xu, Y.; Chang, W. J.; Chen, X. L.; Jin, B. S. CFD modeling of MEA-based CO_2 spray scrubbing with computational-effective interphase mass transfer description. *Chem. Eng. Res. Des.* **2023**, *189*, 606−618.
(48) Kies, F. K.; Benadda, B.; Otterbein, M. Experimental study on mass transfer of a co-current gas−liquid contactor performing under high gas velocities. *Chem. Eng. Process.* **2004**, *43* (11), 1389−1395.
(49) Fu, K.; Sema, T.; Liang, Z. W.; Liu, H. L.; Na, Y. Q.; Shi, H. C.; Idem, R.; Tontiwachwuthikul, P. Investigation of Mass-Transfer Performance for CO_2 Absorption into Diethylenetriamine (DETA) in a Randomly Packed Column. *Ind. Eng. Chem. Res.* **2012**, *51* (37), 12058−12064.
(50) Li, Z.; Ji, X. Y.; Yang, Z. H.; Lu, X. H. Experimental studies of air-blast atomization on the CO_2 capture with aqueous alkali solutions. *Chin. J. Chem. Eng.* **2019**, *27* (10), 2390−2396.
(51) Qiao, Z. H.; Chen, Z. Z.; Gong, H. J.; Wang, Y.; Yu, H. Q.; Chen, L. Carbon dioxide absorption and anti-clogging performance of a novel millimeter-scale channel absorber. *Chem. Eng. Res. Des.* **2023**, *200*, 169−175.
(52) Demontigny, D.; Tontiwachwuthikul, P.; Chakma, A. Parametric studies of carbon dioxide absorption into highly concentrated monoethanolamine solutions. *Can. J. Chem. Eng.* **2001**, *79* (1), 137−142.

https://doi.org/10.1021/acs.iecr.3c04470
Ind. Eng. Chem. Res. 2024, 63, 5618−5628